Generated using the official AMS LATEX template v6.1

Connections between upper tropospheric and lower stratospheric circulation responses to increased CO₂

Molly E. Menzel, a,b Darryn W. Waugh, Clara Orbea

^a NASA Goddard Institute for Space Studies, New York, NY, USA

^b Department of Earth and Planetary Sciences, Johns Hopkins University, Baltimore, MD, USA

Corresponding author: Molly Menzel, molly.menzel@nasa.gov

1

This preliminary Online Release: version has been accepted for publication in Journal of Climate, may be fully cited, and has been assigned DOI 10.1175/ JCLI-D-22-0851.1. The final typeset copyedited article will replace the EOR at the above DOI when it is published.

ABSTRACT: There are a myriad of ways atmospheric circulation responds to increased CO₂. In the troposphere, the region of the tropical upwelling narrows, the Hadley Cells expand, and the upper level subtropical zonal winds that comprise the subtropical jet strengthen. In the stratosphere, the tropical upwelling narrows and strengthens, enhancing the Brewer-Dobson Circulation. Despite the robustness of these projections, dynamical coupling between the features remains unclear. In this study, we analyze output from the NASA Goddard Institute for Space Studies (GISS) ModelE coupled climate model to examine any connection between the upper tropospheric and lower stratospheric circulation by considering the features' seasonality, hemispheric asymmetry, scaling, and transient response to a broad range of CO₂ forcings. We find that a narrowing and strengthening of upper tropospheric upwelling occurs with a strengthening of the subtropical jet. There is also a narrowing and strengthening of lower stratospheric upwelling that is related to an equatorward shift in critical latitude for wave breaking and the associated strengthening of the subtropical lower stratosphere's zonal winds. However, the stratospheric responses display different seasonal, hemispheric, and transient patterns than those in the troposphere, indicating independent circulation changes between the two domains.

1. Introduction

A wide range of changes in zonal-mean atmospheric circulation have been reported as a response to increased atmospheric CO₂. In the troposphere, this includes a widening of the Hadley Cell (HC) (Seidel et al. 2008; Birner et al. 2014), poleward shift of the eddy-driven jet (EDJ) (Barnes and Polvani 2013; Kushner et al. 2001), strengthening and upward shift of the subtropical jet (STJ) (Shaw and Tan 2018; Singh and O'Gorman 2012), and a narrowing of the intertropical convergence zone (ITCZ) (Lau and Kim 2015; Byrne et al. 2018). Likewise, models show that the lower stratospheric circulation also responds to increased CO₂ with a narrowing and acceleration of the Brewer-Dobson Circulation (BDC) (Lin and Fu 2013; Butchart et al. 2006; Eichelberger and Hartmann 2005).

However, there remains uncertainty in the mechanisms of these changes and it is not well known how tightly coupled features are to one another. For example, there has been interest over the last decade in diagnosing tropical widening but, results are dependent on the metrics used to define tropical width (Seidel et al. 2008; Davis and Birner 2017). It has recently been determined that the HC edge is strongly linked to eddy momentum flux convergence such that a poleward shift of the EDJ is associated with HC expansion (Chemke and Polvani 2019; Waugh et al. 2018). In contrast, the strength of the STJ has a contradictory relationship with the HC edge. While a poleward HC is associated with a weaker STJ interannually, the STJ strengthens in response to CO₂ as the HC widens (Menzel et al. 2019). Yet, STJ behavior is still related to HC dynamics as the circulation's poleward advection of angular momentum is an important contribution to STJ strength.

The uncertainty in coupling between different features is especially true between the troposphere and stratosphere. The acceleration of the BDC has been linked to the strengthening of the zonal winds in the subtropical upper troposphere and lower stratosphere (UTLS) via enhanced wave propagation (Garcia and Randel 2008; Shepherd and McLandress 2011). One hypothesis arising from those studies is that the lower stratospheric upwelling inducing the BDC is impacted by the upper tropospheric upwelling through changes in the STJ. It is believed that in addition to the STJ's coupling to the upper tropospheric upwelling through HC dynamics, it is also coupled to the BDC as an extension of the UTLS subtropical winds that moderate wave propagation into the lower stratosphere. Li et al. (2010) note a narrowing of the HC's upwelling branch in the 21st Century in addition to the enhanced lower stratospheric upwelling, and suggested changes in eddy forcing

could be playing a role in both trends. The narrowing of tropical upwelling presented in Li et al. (2010) is consistent with some studies that show the Intertropical Convergence Zone (ITCZ) is narrowing in a changing climate (Byrne et al. 2018), offering a possible connection between the width of the ITCZ and BDC. However, a thorough characterization of the potential links between stratospheric and tropospheric circulations is still lacking. Quantification of these connections is needed to better understand the processes causing changes in different aspects of the circulation, and also to determine if observed changes in one aspect can be used to infer changes in another.

This paper examines the couplings between tropical tropospheric and stratospheric circulation changes in response to CO₂. Which features within and between the two domains are related? We address this question by using a suite of abrupt CO₂ simulations with varying forcing magnitudes in a single global climate model. Our methods are presented in Section 2 and Section 3 considers the zonal-mean response of relevant fields. We then investigate relationships within the individual levels (Sect. 4-5) as well as between them (Sect. 6). Finally, our conclusions and implications are presented in Section 7.

2. Methods

This study analyzes output from the NASA Goddard Institute for Space Studies (GISS) E2.1-G comprehensive global climate model (Kelley et al. 2020) that contributed to the Coupled Model Intercomparison Project, Phase 6 (CMIP6) (Eyring et al. 2016). The atmosphere component, fully coupled to ocean, land, and sea ice components, has 40 vertical levels reaching up to about 0.1 hPa, a horizontal resolution of 2° latitude x 2.5° longitude, and includes background fields of ozone and aerosol concentrations derived from fully interactive chemistry models (Bauer et al. 2020). We examine a total of seven 150-year-long simulations; one control simulation forced with preindustrial emissions levels, and six forcing simulations that instantaneously perturb the atmospheric CO₂ with varying degrees of magnitude (2xCO₂, 3xCO₂, 4xCO₂, 5xCO₂, 6xCO₂, 8xCO₂). In addition to the fully coupled integrations, we also examine the results from 30-year-long simulations using prescribed pre-industrial SSTs traditionally used to estimate effective radiative forcing. Here, we use these integrations to distinguish between the rapid radiative versus temperature mediated responses in various measures of the circulation. This novel suite of simulations provides unique insight into how climate features respond to forcing beyond that of the typical quadrupling of CO₂.

In fact, Mitevski et al. (2021) use the simulations to demonstrate that not all circulation features have a linear response to CO₂. Not only do we use it to consider how features' responses scale with CO₂ magnitude, it also provides a measure of robustness.

a. Metrics

All metrics used in this study are visualized by the tropospheric and stratospheric climatological circulation shown in Figure 1. To diagnose the upper tropospheric upwelling, we first take the vertical average of the meridional streamfunction between 100 and 300 hPa and find where it crosses zero and is maximized and minimized north and south of that zero crossing, respectively. Physically, the latitude of zero crossing distinguishes between the Northern Hemisphere's (NH) and Southern Hemisphere's (SH) circulation cells and the extrema identifies the boundary between upward and downward vertical motion. The upwelling's hemispheric width, ϕ UP_{TROP}, is determined by the distance between the meridional streamfunction extrema and its zero crossing. Similarly, the strength of the upwelling, ψ UP_{TROP}, is calculated as the magnitude of the vertically averaged upper tropospheric streamfunction at its extrema. To define the poleward extent, or edge, of the HC, ϕ HC, we use the "PSI_500" metric via the TropD python package (Adam et al. 2018).

Our lower stratospheric upwelling metrics are instead derived from the residual streamfunction at 70 hPa, consistent with previous literature (Rosenlof 1995; Butchart et al. 2006; Seviour et al. 2012). The lower stratospheric upwelling width, ϕ UP_{STRAT} is calculated as the latitude of the residual streamfunction's extrema, known as the "turnaround latitude," and the lower stratospheric upwelling strength, ψ UP_{STRAT} is defined as the magnitude of the residual streamfunction at its extrema. Although previous studies mentioned above consider lower stratospheric upwelling metrics across the entire tropics, we use metrics that distinguish between hemispheres to allow for seasonal and hemispheric analysis.

To diagnose STJ behavior, we calculate an "adjusted wind" field where the zonal-mean zonal wind at 850 hPa is subtracted from the zonal-mean zonal wind vertically averaged from 100 to 400 hPa (Waugh et al. 2018). We then define the strength of the STJ, uSTJ, as the value of the adjusted wind field at its most equatorward peak using a quadratic fit, as in Menzel et al. (2019). We define an additional subtropical zonal wind metric, U_{25} , as the magnitude of the zonal winds at 25° N/S, vertically averaged from 70 to 100 hPa. This metric is useful in representing the lower stratospheric

subtropical zonal winds as uSTJ is limited to the upper troposphere. To diagnose stratospheric behavior, we also consider a critical latitude metric, ϕU_0 , defined by the latitude at which the zonal wind is zero at 70 hPa, consistent with the other stratospheric metrics. Since stationary waves only

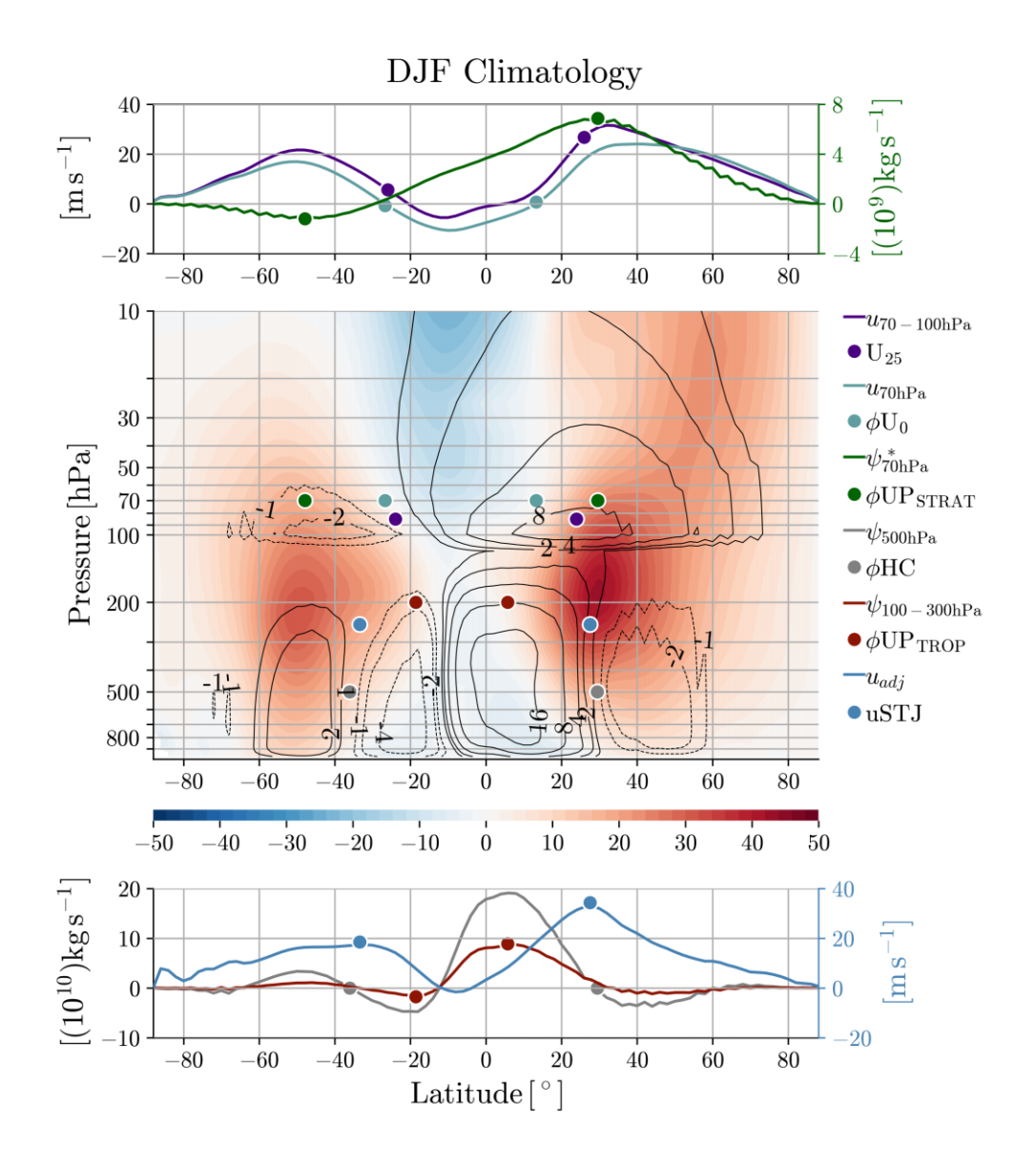


Fig. 1. Zonal-mean DJF climatology of zonal wind (colored contours, $[m\,s^{-1}]$) and meridional streamfunction (black contours, $[(10^{10})\,\mathrm{kg}\,\mathrm{s}^{-1}]$ below 100 hPa, residual above $[(10^9)\,\mathrm{kg}\,\mathrm{s}^{-1}]$) as well as zonal wind at 70 hPa (top, aqua), residual streamfunction at 70 hPa (top, green), lower stratospheric zonal winds (top, purple), adjusted wind (bottom, blue), upper tropospheric meridional streamfunction (bottom, pink), and meridional streamfunction at 500 hPa (bottom, grey). Circles represent the metrics calculated from the associated latitudinal fields.

propagate in westerly zonal flow, the latitude where zonal flow is zero acts as a boundary for wave propagation (Hardiman et al. 2014). True wave breaking occurs just poleward of this latitude in weak westerly zonal wind, but the zero crossing for zonal wind is a good approximation.

For all metrics defined by local extrema of relevant fields, we first locate the extrema and then apply a quadratic fit to the field with a latitudinal resolution of 0.1°. Our metrics are then defined by the maximum value of that quadratic fit.

b. Approach

In order to determine which circulation changes are caused by the same processes, we examine their 1) seasonality, 2) hemispheric differences, 3) scaling with forcing magnitude, and 4) response time to a range of abrupt CO₂ levels. Here, we define changes as the difference between the forcing simulations and the control simulation with pre-industrial emissions, calculating the steady state response as the average over the last 50 years of each simulation. If two circulation features are dynamically coupled, their metrics will respond to CO₂ consistently across all four types of analysis. Otherwise, the features' behaviors are set by different physical mechanisms. For instance, two metrics may have corresponding steady state responses to CO₂ which suggest a possible connection yet, incompatible time scales of that response reveal they are responding to different processes. This is the case for the STJ strength and HC edge (Menzel et al. 2019). On the other hand, temporal response analysis can further solidify a result that two features have a direct link, as is done in Chemke and Polvani (2019) and Grise and Polvani (2017) to connect the HC edge to eddy momentum flux convergence.

Using a broad analysis perspective that includes seasonality, hemispheric difference, CO₂ scaling, and response time to forcing is an underutilized approach to discovering connections between circulation features. We first apply this method to relationships in the troposphere, do the same for the stratosphere, then ultimately for troposphere-stratosphere interaction.

3. Zonal-Mean Changes

Before analyzing the above metrics, we first consider the patterns of change in relevant zonal-mean fields based on CO_2 forcing. The responses to $4xCO_2$ for the December-January-February (DJF) and June-July-August (JJA) seasons are displayed in Figure 2. Despite noteworthy nonlinearity of

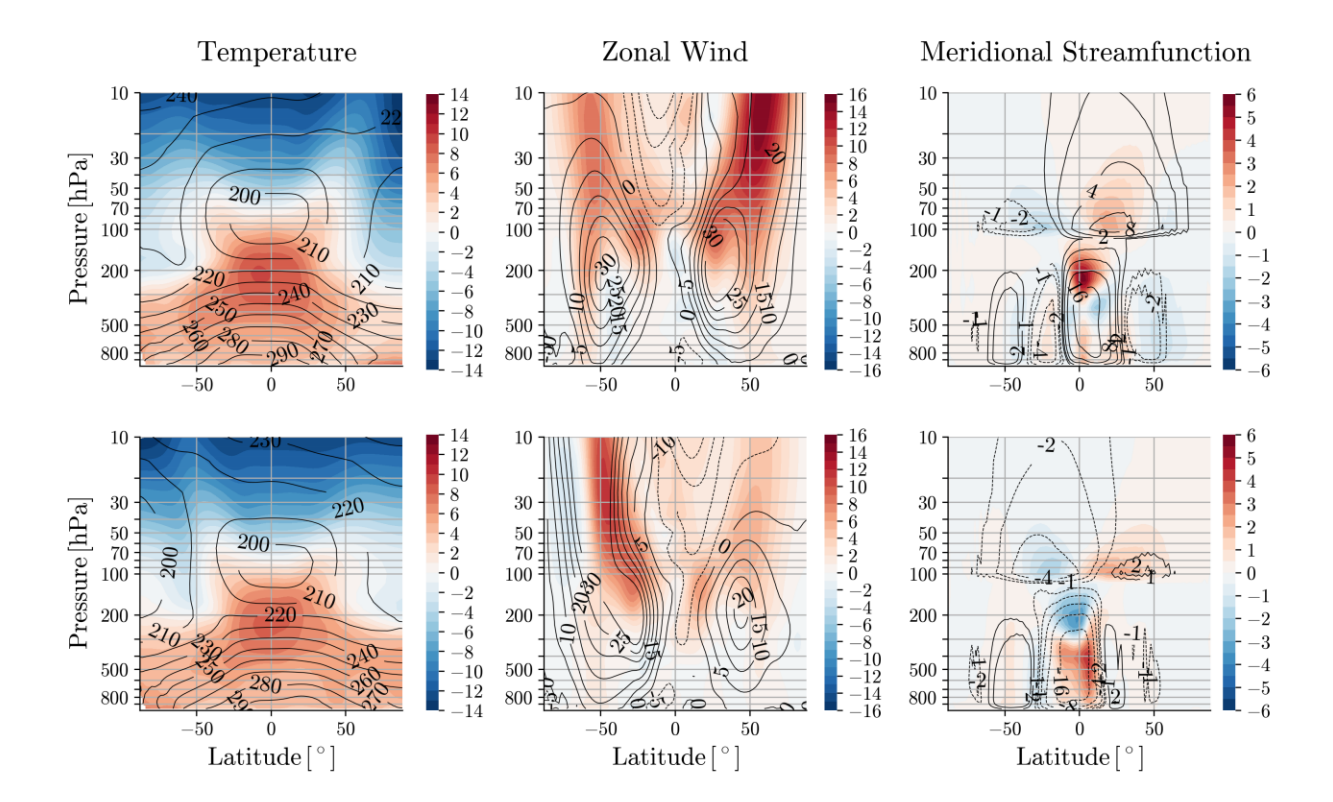


Fig. 2. Zonal-mean climatology (black contours) and response (colored shading) of temperature (left, [K]), zonal wind (center, [m s⁻¹]), and meridional streamfunction (right, [(10^{10})kg s⁻¹] below 100 hPa, residual above [(10^9)kg s⁻¹]) to 4xCO₂ for DJF (top) and JJA (bottom) seasons.

some circulation features' response to CO₂ forcing (Mitevski et al. 2021), the patterns of change in Figure 2 are broadly similar across forcing magnitudes (see Figs. S3-S4). As a result, focusing on the 4xCO₂ output in this section is representative of the simulations.

As shown in previous studies, there is a warming of the troposphere, amplified in the tropical upper troposphere consistent with multi-model output (Shaw 2019; Menzel et al. 2019), and increased cooling of the stratosphere with height (Garcia and Randel 2008; Chrysanthou et al. 2020). There is slight indication that the upper tropospheric warming is maximized in the summer hemisphere, and the cooling descends to lower levels in the winter vs summer pole. Otherwise, the temperature response appears hemispherically symmetric.

In the subtropical troposphere, we see a strengthening and upward shift of the STJ where the wind response is maximized just above 100 hPa (Shaw 2019). Below 300 hPa, there is negligible change. This contrasts with the midlatitudes where the strengthening of zonal winds

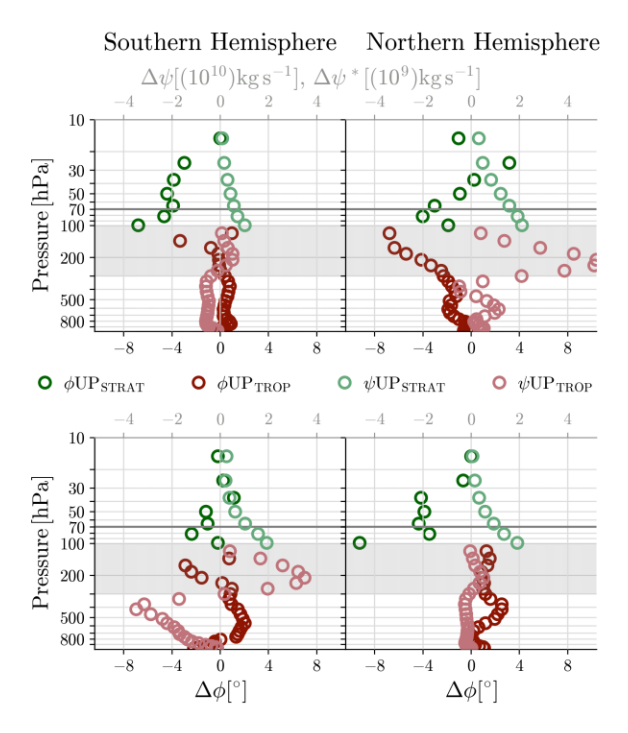


Fig. 3. Response of the tropospheric (below 100 hPa) and lower stratospheric (above 100 hPa) upwelling width and strength to $4xCO_2$ for DJF (top) and JJA (bottom) seasons. The shaded region between 100-300 hPa shows the tropospheric level range at which ϕUP_{TROP} and ψUP_{TROP} are calculated. Likewise, the horizontal line at 70 hPa shows the level at which ϕUP_{STRAT} and ψUP_{STRAT} are found. Note, positive values for change in ϕUP_{STRAT} reflect a poleward shift.

nearly reaches the surface and indicates a shift in the EDJ (Kushner et al. 2001). There is also prominent strengthening of the westerlies in the tropical lower stratosphere and at all levels of the stratosphere's midlatitudes (Shepherd and McLandress 2011). With that said, the largest strengthening of westerlies occurs in the stratospheric winter season.

The most interesting changes in the meridional streamfunction occur in the tropical troposphere. In both winter seasons, there is a strong increase in streamfunction above 300 hPa consistent with the multi-model analysis in Menzel et al. (2019). However, JJA winter shows a near equal decrease in magnitude of its streamfunction below 300 hPa whereas the change below 300 hPa in DJF winter is negligible. In either summer hemisphere, there is little to no change in the streamfunction. In the tropical stratosphere, changes in the streamfunction are consistent with a narrowing and

strengthening of the upwelling apparent in individual models (Orbe et al. 2020) and multi-model output (Abalos et al. 2020).

The vertical dependence of the tropical upwelling response is shown in Figure 3. In most cases, the response in the upper troposphere opposes that of the mid-to-lower troposphere for both the width and strength of upwelling. The only exceptions are NH DJF where the upwelling narrows and strengthens throughout the whole troposphere and NH JJA where the upwelling widens at all levels. Note, the lack of opposing sign in the NH winter compared to SH winter may be a model dependent result. Additionally, a strengthening of upwelling coincides with its narrowing and vice versa. There is also notable seasonality of the tropospheric upwelling such that the winter seasons show a more prominent response in upwelling than the summer seasons. Similar seasonality is not apparent in the stratospheric upwelling as it shows more consistent response between winter and summer. In light of the upwelling response's vertical dependence, studies may be mindful of their choice of level in diagnosing the tropical upwelling and define their metrics according to the physical mechanisms of focus. Here, our focus is on the upper tropospheric dynamics and thus we consider the 100-300 hPa level.

4. Tropospheric Connections

Having shown changes in a range of tropospheric circulation features, we now examine the connections between these responses to increased CO₂. As previously shown in Figure 2, there is a warming and increase in streamfunction in the tropical upper troposphere. The steady state changes in tropospheric metrics are shown in Figure 4.

Consistent with Figure 2, ϕ HC shifts poleward consistently across seasons and hemispheres. We also see that generally, a larger CO₂ forcing prompts a larger poleward shift. In contrast, ϕ UP_{TROP} shifts equatorward indicating a narrowing of the upper tropospheric upwelling. The only exception is JJA, where there is a slight poleward shift, possibly occurring as a result of the summer Asian monsoon. Although a northern hemispheric feature, the summer Asian monsoon impacts zonal-mean upwelling that contributes to both the summer and winter cells. Thus, ϕ UP_{TROP} may be equally sensitive to the monsoon in SH JJA as NH JJA. Not only do ϕ HC and ϕ UP_{TROP} respond in the opposite direction, ϕ UP_{TROP} shows stronger seasonality than ϕ HC, particularly in the NH, whereby its response is large in the winter and spring but negligible in the summer and

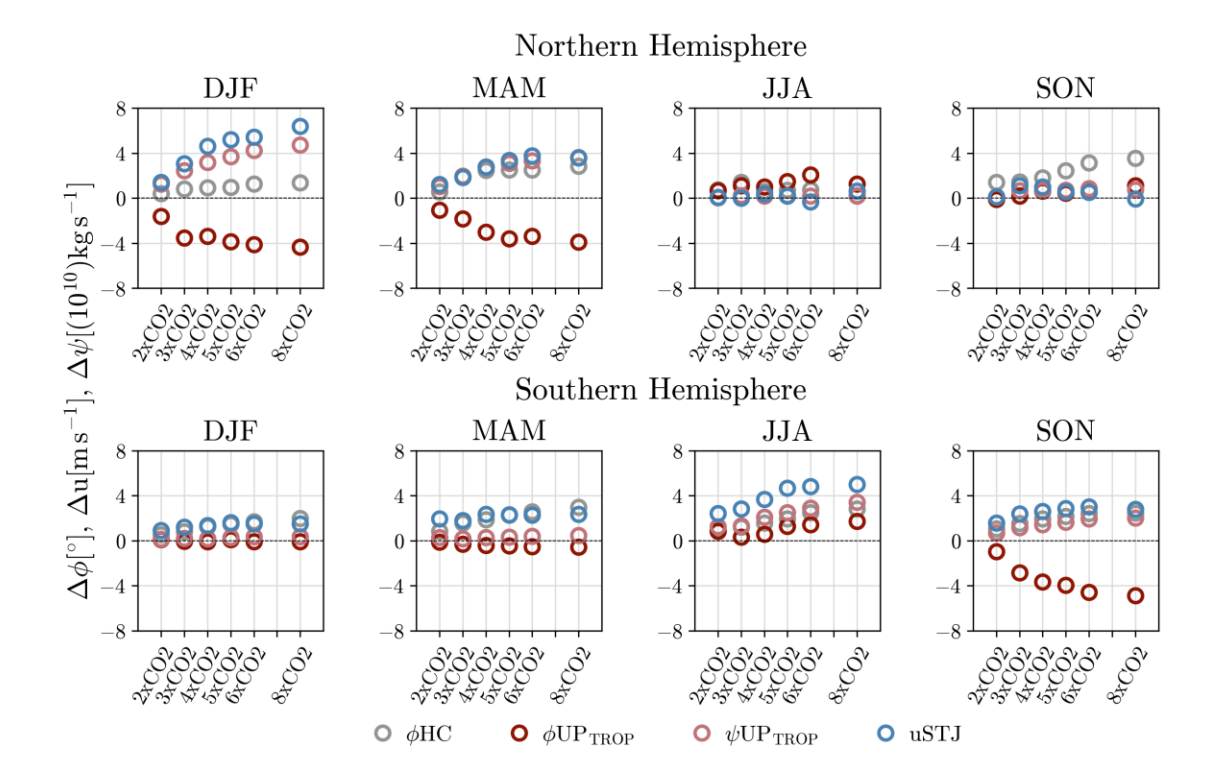


Fig. 4. Steady state response of tropospheric metrics for each season and simulation.

fall. ϕ UP_{TROP} also differs from ϕ HC in that it shows a much broader range of responses across the CO₂ forcing magnitudes in NH DJF and MAM.

The notable seasonality of ϕUP_{TROP} is also apparent in the response of ψUP_{TROP} . ψUP_{TROP} strengthens in the winter and spring seasons but has a minimal response to forcing in summer and fall. Additionally, the NH response of ψUP_{TROP} is larger than its SH response by about a factor of two. In the seasons and hemispheres where ψUP_{TROP} 's response is largest, we see it scale with CO_2 magnitude such that a larger forcing invokes a larger strengthening.

The strengthening and narrowing of upper tropospheric upwelling occurs with a strengthening and upward shift of the subtropical upper tropospheric winds. The seasonal and hemispheric patterns of response in ϕUP_{TROP} and ψUP_{TROP} appears in uSTJ as well; its strengthening is largest in the winter, reduced in the summer and fall, and the NH winter response is relatively larger than the SH winter response. Like ϕUP_{TROP} , uSTJ also shows varied responses across CO_2 forcings. There is generally a larger strengthening of uSTJ for larger CO_2 , but interestingly, that scaling appears to plateau at higher forcing levels.

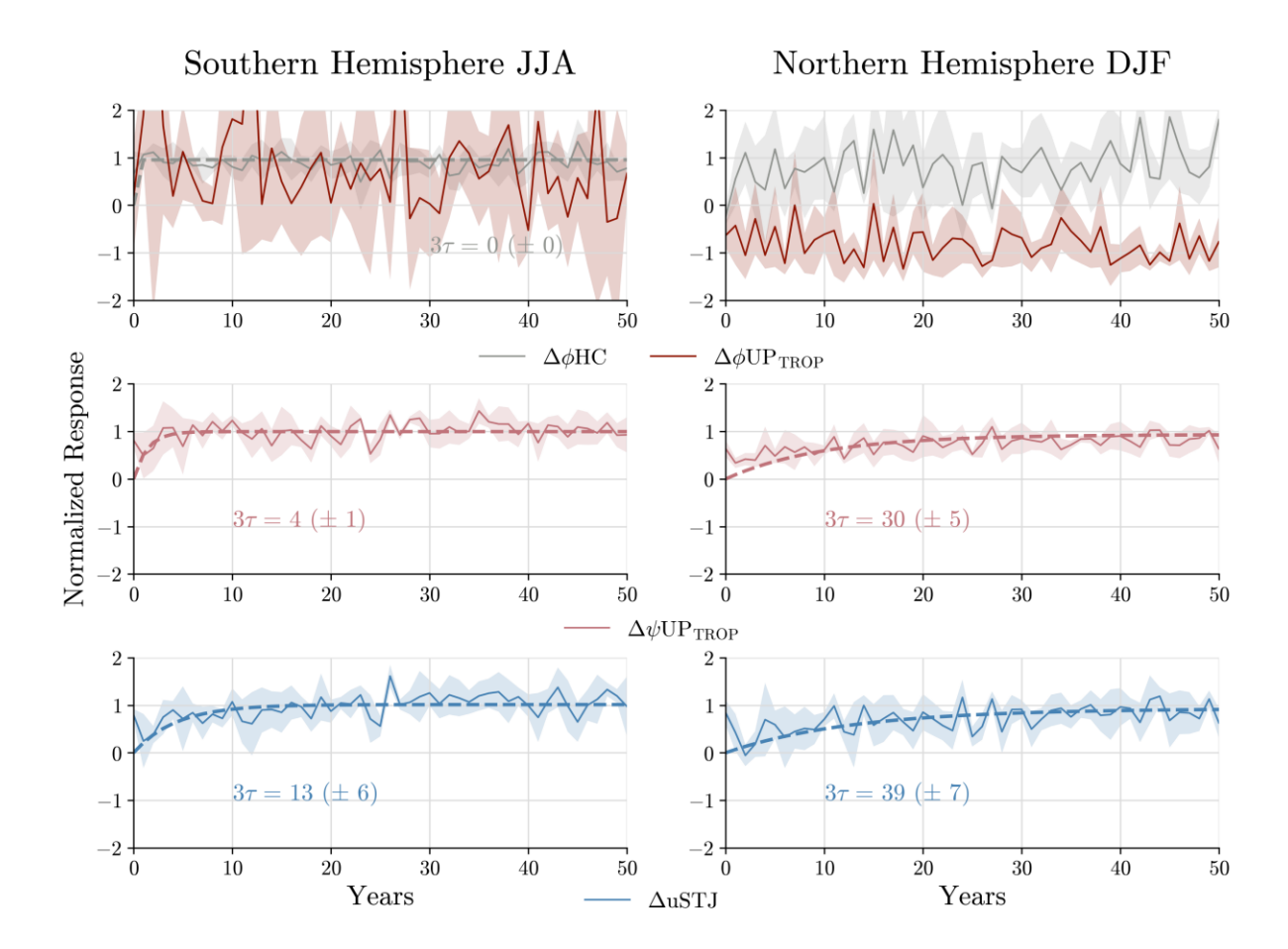


Fig. 5. Time series of tropospheric metrics' simulation-mean transient responses to CO_2 using those simulations with forcing greater than $4xCO_2$, normalized by their steady state response, for SH JJA (left) and NH DJF (right). For each metric, the shading indicates one standard deviation of simulation spread and the dashed line shows the exponential fit. The time scale of response, 3τ is listed for each metric along with the standard deviation of 3τ across individual simulations in parentheses.

From the steady state analysis, we find a coupling between the responses of ϕ UP_{TROP}, ψ UP_{TROP}, and uSTJ. This is supported by their similar seasonality, hemispheric differences, and scaling with CO₂ levels. However, these metrics are uncoupled from ϕ HC's response which has more limited seasonality, less hemispheric asymmetry, and a more narrow range of CO₂ forcing responses.

To examine the metrics' transient response to CO₂, we normalize each response by its steady state change and calculate the simulation-mean transient response (Fig. 5). Here, we focus our analysis on the winter season when the largest response of all metrics occurs, but the metrics' transient response for all seasons and hemispheres is included in the Supporting Information (see

Figs. S9-S16). Note, there is large uncertainty in the transient response analysis. One source is that certain metrics, or certain seasons or simulations, have large interannual variability, making it difficult to infer any conclusions from their transient response to CO_2 . This is true for ϕUP_{TROP} , but it also applies to all metrics in $2xCO_2$ and $3xCO_2$, where their steady state changes are small. For this reason, we exclude the $2xCO_2$ and $3xCO_2$ simulations from all transient response analysis. Another inadequacy is that taking the normalized simulation-mean of the metrics' transient response assumes a linearity across all CO_2 forcings, which may not be the case for all metrics. In fact, Mitevski et al. (2021) already show that ϕHC 's steady state response to CO_2 is non-linear, but it is unknown how the time scale for response varies with CO_2 forcing. Lastly, there are discrepancies in the quality of exponential fit to the transient responses, so we caution the emphasis given to the time scale quantification, see below. Even with these limitations, the transient response analysis does present useful insights into the features' responses to CO_2 .

Within the NH DJF season, ψ UP_{TROP} and uSTJ respond to CO₂ with similar time scales. Interestingly, both metrics have a quicker response in SH JJA. In contrast, ϕ HC responds near instantaneously in SH JJA. This result is consistent with Chemke and Polvani (2019) and Menzel et al. (2019) who both show the ϕ HC's short response is compatible with that of the latitude of maximum eddy momentum convergence. The large interannual variability of ϕ HC in NH DJF and ϕ UP_{TROP} in both winter seasons makes it difficult to interpret their transient responses.

To be more precise, we quantify the time scales of response. To do so, we fit the normalized and simulation-mean transient response to an exponential function of the form

$$f(t) = a(1 - e^{-t/\tau})$$

where a is a constant, t is the time in years, and τ is the time constant. Our time scale is then given by 3τ , when the exponential fit reaches 95% of its normalized steady state solution. These values are listed in Figure 5. Although 3τ is useful for comparison, the exponential function is an adequate yet imperfect fit to some metrics' transient response. Additionally, we calculate the 3τ for each simulation's individual transient response and find the standard deviation of 3τ across simulations. This value is included in parentheses next to 3τ in Figure 5 to present a measure of uncertainty in time scales across simulations. Note, we don't perform the exponential fit for metrics whose interannual variability is larger than their steady state normalized and simulation-mean response,

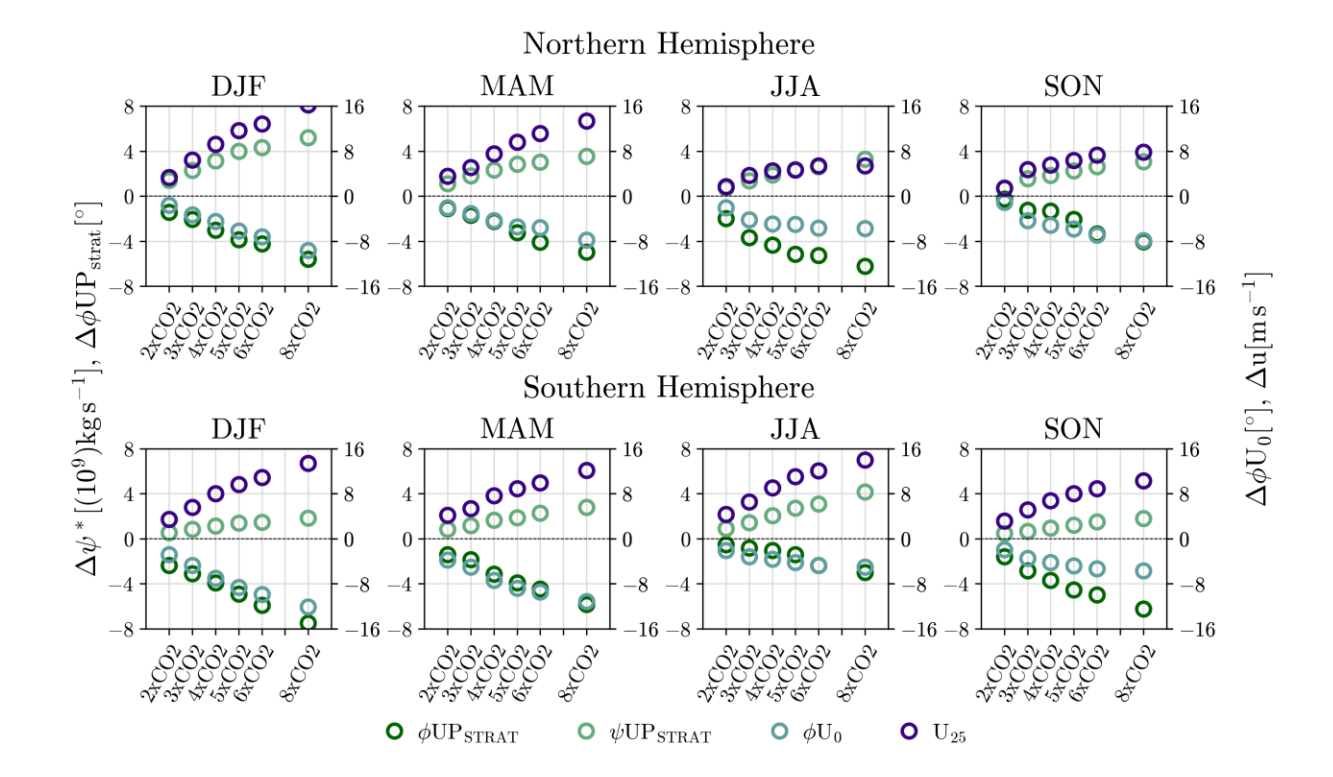


Fig. 6. Steady state response of stratospheric metrics for each season and simulation. Note, positive values for change in ϕ UP_{STRAT} reflect a poleward shift.

or if the uncertainty in 3τ is greater than the time scale itself. By calculating 3τ , we confirm that in NH DJF ψ UP_{TROP} and uSTJ respond with an intermediate time scale of around 40-50 years. This time scale reduces to 4 and 13 years for ψ UP_{TROP} and uSTJ, respectively in SH JJA. Starkly, ϕ HC responds rapidly in SH JJA, within the first year.

Altogether, our analysis shows that the upper tropospheric upwelling is strongly coupled to the subtropical jet in their responses to CO_2 . Both exhibit large seasonality such that their responses are larger in the winter and spring than the summer and fall, similar hemispheric asymmetry as the NH response is about twice that of the SH response, and comparable time scales in response to CO_2 .

5. Stratospheric Connections

We continue by performing the same analysis with the stratospheric metrics. As discussed in Section 3, the stratospheric response to CO₂ is a cooling that increases with height, an increase

in zonal winds particularly in the winter season, and an acceleration of the meridional residual circulation (Fig. 2). Figure 6 confirms these qualitative results by showing the stratospheric metrics' steady state responses.

There is strengthening of the subtropical lower stratospheric winds shown by the increase in U_{25} . Note, this response shows seasonality only in the NH, where the increase is largest in the winter and smallest in the summer. However, its response is more consistent across seasons in the SH. It also appears that the response of U_{25} scales linearly with CO_2 , increasing upwards of 16 ms⁻¹.

A strengthening of the lower stratospheric subtropical winds is accompanied by an equatorward shift in the critical latitude, as shown by the negative sign of the ϕU_0 response. Interestingly, and in opposition to the pattern of U_{25} response, the largest seasonality of ϕU_0 is in the SH while its NH response is consistent across seasons. Also, the SH seasonality indicates that the largest ϕU_0 response is in the summer and fall seasons. ϕU_0 is also similar to U_{25} in that it scales nearly linearly with CO_2 level.

There is also an equatorward shift of ϕUP_{STRAT} , shown by its negative sign, which indicates a narrowing of the lower stratospheric upwelling. Its response only shows subtle seasonality with a slightly larger response in the summer seasons than the others. Additionally, the response is fairly symmetric between hemispheres and, similar to U_{25} and ϕU_0 , responds linearly with forcing magnitudes.

Lastly, the lower stratospheric upwelling strengthens, seen by the increase in ψ UP_{STRAT}. Although seasonality is slight, its largest increase is in the winter seasons. Similar to ϕ UP_{STRAT}, ψ UP_{STRAT}'s response is consistent between hemispheres. Its linearity with CO₂ is less obvious but it shows a general increase in response given a larger forcing.

Altogether, the steady state responses of U_{25} , ϕU_0 , ϕUP_{STRAT} , and ψUP_{STRAT} indicate that they are all coupled together. All show limited seasonality, comparable responses between hemispheres, and nearly linear changes with CO_2 forcing.

This conclusion is further solidified when looking at the stratospheric metrics' simulation-mean transient response to CO_2 in Figure 7 (again excluding the $2xCO_2$ and $3xCO_2$ simulations for reasons stated in Section 4). Most metrics show a range of response time scale between 10-30 years. One exception is ψUP_{STRAT} which responds within 8 years in SH JJA but 13 years in NH DJF. In NH DJF, ϕUP_{STRAT} 's time scale of 16 years is more closely related to ψUP_{STRAT} than it

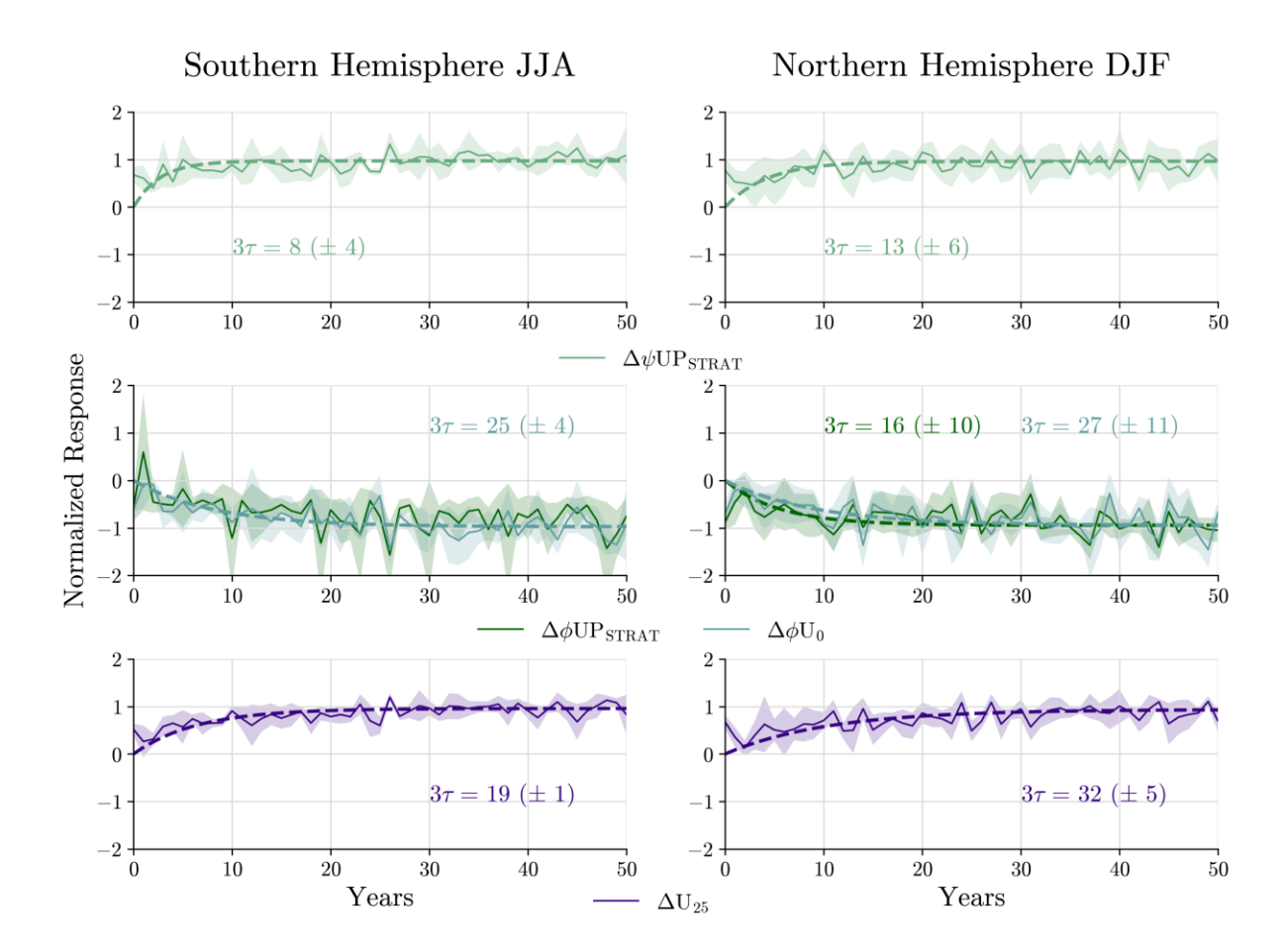


Fig. 7. Time series of stratospheric metrics' simulation-mean transient responses to CO_2 using those simulations with forcing greater than $4xCO_2$, normalized by their steady state response, for SH JJA (left) and NH DJF (right). For each metric, the shading indicates one standard deviation of simulation spread and the dashed line shows the exponential fit. The time scale of response, 3τ is listed for each metric along with the standard deviation of 3τ across individual simulations in parentheses. Note, positive values for change in ϕUP_{STRAT} reflect a poleward shift.

is to ϕU_0 . Of all metrics, ϕU_0 's time scale is most consistent between SH JJA and NH DJF. Like ψUP_{STRAT} , U_{25} 's response is quicker in SH JJA than NH DJF, resembling similar time scales as uSTJ (Fig. 5), but stays within the 10-30 year time range.

The transient response of ψ UP_{STRAT} is distinct from the other stratospheric metrics in that it reaches its steady state response within 10 years in SH JJA. Although having a slightly longer time scale of 13 years in NH DJF, it still shows a materially quicker response than ϕ U₀ and U₂₅ in the same season. A possible cause of this quick time scale is that the stratospheric upwelling

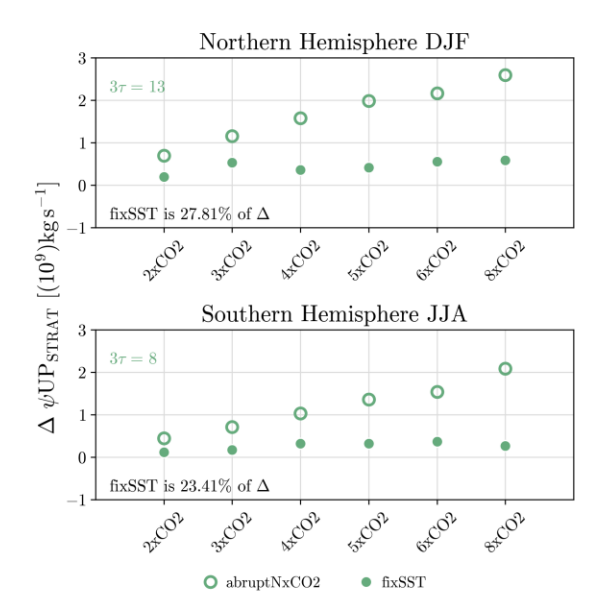


Fig. 8. The steady state response of ψUP_{STRAT} to CO_2 with fixed sea surface temperatures (SST) and a fully coupled ocean for the winter seasons. The time scale of response, 3τ is listed in addition to the percentage of coupled steady state response that is due to a rapid CO_2 adjustment.

strength is uniquely impacted by the deeper branch of the BDC. In decomposing the BDC response, Chrysanthou et al. (2020) reveals that half of the deep BDC circulation increase occurs as a rapid adjustment (i.e. a direct result of CO₂ increase) regardless of the global mean SST warming. In contrast, a rapid adjustment only accounts for 20% of the shallow BDC response (Orbe et al. 2020).

To verify this result, Figure 8 compares ψ UP_{STRAT}'s steady state response to CO₂ in the fully coupled configuration with that of the same forcing while sea surface temperature (SST) are held fixed. As in Chrysanthou et al. (2020), the fixed SST configuration reveals the atmosphere's rapid adjustment to CO₂ forcing, a response dependent on the CO₂ increase alone, and is characterized by stratospheric cooling and minimal temperature change in the troposphere. We find that in the winter seasons, the fixed SST response of ψ UP_{STRAT} accounts for over 20% of its coupled response. Indeed, this supports the result that the rapid adjustment of the BDC deep branch, accounting for a large portion of its response, plays a role in the response of ψ UP_{STRAT} via downward control. Haynes et al. (1991) first described the downward control method as how the tropical upward mass flux is influenced by dissipating Rossby and gravity waves. To satisfy mass continuity, the upward mass flux at lower latitudes must be balanced by the extratropical downward mass flux which is

determined by that wave activity (Haynes et al. 1991; Rosenlof and Holton 1993). Although this addresses how the ψ UP_{STRAT} response time is within 5-15 years for both hemispheres, it falls short of explaining why ϕ UP_{STRAT} has the same time scale in NH DJF.

In summary, the stratospheric metrics show consistent patterns in response to CO_2 . For all, there is limited seasonality and no obvious differences between the hemispheres. Physically, a narrower and stronger lower stratospheric upwelling is associated with a more equatorward critical latitude for wave breaking and stronger lower stratospheric subtropical winds. The one part of analysis that deviates from a strong coupling is that of the transient response to CO_2 , where ψUP_{STRAT} responds materially faster than ϕU_0 , and U_{25} in SH JJA. This result likely arises from ψUP_{STRAT} 's sensitivity to the deeper branch of the BDC, which adjusts rapidly to 4xCO2 forcing.

6. Tropospheric-Stratospheric Interactions

Having shown strong coupling in circulation features within the troposphere and stratosphere, we now investigate possible physical connections between them. Doing so examines the hypothesis that the upper tropospheric upwelling is dynamically tied to the lower stratospheric upwelling via the STJ and UTLS subtropical winds (Sect. 1).

Generally, the upper tropospheric and lower stratospheric upwellings share the same response to CO_2 ; both narrow and strengthen. Further, the strengthening of the subtropical winds in the upper troposphere and lower stratosphere is robust. However, there are notable differences between the responses of the tropospheric and stratospheric metrics. First, there is stronger seasonality in the tropospheric metrics' response than that of the stratospheric metrics. In particular, ϕUP_{TROP} , ψUP_{TROP} and uSTJ show a larger response in the winter and spring than the summer and fall. In contrast, the responses of ϕUP_{STRAT} , ψUP_{STRAT} , ϕU_0 , and U_{25} have weak seasonality. The only slight connection is the seasonality of U_{25} 's response in the NH, but then its lack of seasonality in the SH response reflects that of all the other stratospheric metrics. Further, the seasonality of U_0 , only present in the SH, is a larger response in the summer and fall than winter and spring, opposing the seasonal pattern of the tropospheric metrics.

Additionally, there are apparent hemispheric differences in response of the tropospheric metrics. The responses of ϕUP_{TROP} , ψUP_{TROP} and uSTJ are larger in the NH than the SH by a factor of

two. Yet, there are no corresponding hemispheric differences in the response of the stratospheric metrics.

Generally, the scaling of response to CO₂ does not easily distinguish between the tropospheric and stratospheric metrics. Although the stratospheric metrics' linear responses with CO₂ forcing seem more obvious, all metrics, even in the troposphere, have a larger response given a larger CO₂ magnitude.

Lastly, there is inconsistency in the time scale of response between the metrics of each domain. In the troposphere, ϕ UP_{TROP}, ψ UP_{TROP} and uSTJ respond in 40-50 years in NH DJF and more quickly in SH JJA. This is slightly slower in NH DJF and slightly quicker in SH JJA than the response of ψ UP_{STRAT}, ϕ UP_{STRAT}, ϕ U0, and U25, which is between 10-30 years for both hemispheres.

These distinctions between the upper tropospheric and lower stratospheric responses are more apparent for the metrics derived from the mean meridional streamfunction than those derived from the zonal-mean zonal wind (see Figures S5-S8 in Supporting Information). Although uSTJ shows stronger seasonality than U_{25} in its steady state response to CO_2 , U_{25} does show some seasonality in the NH, where its response is reduced in summer and fall. Additionally, both metrics strengthen with similar times scales, within 20 years in SH JJA and after 30 years in NH DJF. Even so, these seasonal and hemispheric patterns are not seen in ϕU_0 's steady state or transient response.

Given this analysis, we find that if any connection between upper tropospheric and lower stratospheric upwelling exists, it is subtle and perhaps inferior to other response processes. Although zonal winds in the broader subtropical UTLS region increase, the pattern of response shown by the STJ does not appear to fully encapsulate the zonal wind increase that impacts the lower stratospheric upwelling. Rather, the zonal wind changes below the tropopause may be distinct from the lower stratospheric level that is connected to the lower stratospheric upwelling. Indeed, there appears a strong coupling between the narrowing and strengthening of the upper tropospheric upwelling and the STJ's strengthening. This, however, is distinct from the lower stratospheric level, where the zonal winds also increase, both the critical latitude of wave breaking and the residual circulation's turnaround latitude shift equatorward, and the lower stratospheric upwelling strengthens.

7. Concluding Remarks

This study investigates connections between tropical circulation changes in response to CO₂ within the troposphere, within the stratosphere, and between the two domains. We find that in the upper troposphere, the tropical upwelling narrows and strengthens with increased CO₂. However, this result is level-dependent and opposes the response of upwelling in the mid-to-lower troposphere. The narrowing and strengthening of the upper tropospheric upwelling occurs with a strengthening of the STJ due to an increase in the circulation's poleward advection of angular momentum (Sect. 4). All features in the upper troposphere show consistent seasonality, hemispheric difference, and scaling with CO₂; their responses are larger in the winter and spring than summer and fall, their NH response is double that of the SH, and they show a broad range of changes with varying CO₂ levels. Further, their responses reach steady state in about 40-50 years in NH DJF and within 15 years in SH JJA.

In the stratosphere, an enhancement and narrowing of the lower stratospheric upwelling is related to a more equatorward turnaround latitude. This corresponds to an equatorward shift of the critical latitude due to an increase in the subtropical lower stratospheric zonal winds (Sect. 5). The responses of all features exhibit minimal seasonality and are consistent across hemispheres. Also, the equatorward shift of the turnaround latitude and critical latitude respond in about 10-30 years along with the strengthening of the subtropical lower stratospheric zonal winds. The strengthening of the stratospheric upwelling happens on a similar time scale in NH DJF, but has a quicker response of 8 years in SH JJA. Its relatively quick transient response is explained by its sensitivity to the BDC's deeper branch.

When considering tropospheric-stratospheric interaction, we find distinct behavior in the responses of the tropospheric and stratospheric features. The strong seasonality of the tropospheric metrics' response is not apparent in that of the stratospheric metrics, the responses of stratospheric metrics are consistent between hemispheres which opposes the hemispheric asymmetry in that of the tropospheric metrics, and the stratospheric metrics' time scale of response is quicker than the tropospheric metrics in NH DJF, but slower in SH JJA. This all implies that despite a strengthening of zonal winds in the broader subtropical UTLS region, the zonal wind response impacting the STJ and connected to the upper tropospheric upwelling may be occurring independently of the zonal wind response impacting the lower stratospheric upwelling. So there is strong coupling of

circulation metrics within the troposphere, and likewise a coupling of circulation metrics within the stratosphere, but evidence of any dynamical connection between the two is lacking.

Such a conclusion may be surprising as it reveals a deficiency in the commonly proposed mechanism for BDC acceleration, that is the strengthening of the STJ (Sect. 1). Additionally, it refutes the hypothesis of a coupling between changes in the upper tropospheric and lower stratospheric upwelling through the STJ response. The STJ's behavior is in fact tied to the upper tropospheric upwelling, but its dynamical connection to the lower stratospheric upwelling is less direct. Altogether, this study cautions against inferring changes in one feature based on another. For example, an observed narrowing of the HC's upwelling does not necessarily mean that the BDC is narrowing as well. Additionally, a strengthened STJ does not imply a strengthening of the UTLS subtropical winds or BDC acceleration. Indeed, these various aspects of circulation all respond to increased CO₂, but comprehensive analysis must be done to prove a strong coupling between the features of interest before such inferences can be made.

Since this study only considers one global climate model, we are constrained in determining the robustness of the conclusions presented. However, some important results are compatible with previous studies that offer multi-model analysis. For instance, the strengthening of the upper tropospheric tropical upwelling is supported by analysis of multi-model CMIP5 response to $4xCO_2$ (Menzel et al. 2019), and multiple chemistry climate models' trends over the 21st Century (Abalos et al. 2020). Similarly, Byrne et al. (2018) reveal that most CMIP5 models produce a narrowing of the ITCZ in the RCP8.5 forcing scenario. Menzel et al. (2019) also confirms that the strengthening of the STJ in response to $4xCO_2$ with a moderate time scale of about 40 years is also a robust result across CMIP5 coupled climate models. Lastly, the narrowing and strengthening of upwelling in the lower stratosphere is robust across CMIP5 (Hardiman et al. 2014) and CMIP6 models (Abalos et al. 2021), as is the equatorward shift in the critical latitude (Hardiman et al. 2014).

Another limitation of the analysis is distinguishing the physical processes responsible for the coupled responses we note. For instance, what is causing the narrowing and strengthening of the upper tropospheric upwelling and coupled STJ strengthening, and why is the response larger in the winter than the summer? It is possible that this is a response to the upper tropospheric warming that occurs with increased CO₂. Such a warming combined with the extratropical cooling in the lower stratosphere increases the meridional temperature gradient in the subtropics which would

act to strengthen the STJ. Also, the larger changes in the winter compared to the summer could be related to a climatologically steeper tropopause break in subtropical winter. Indeed, the zonal wind profile does maintain thermal wind balance, but it is difficult to interpret any causality in that relationship. Is the upper tropospheric warming setting the meridional temperature gradients, thus strengthening the upper tropospheric subtropical winds, and subsequently enhancing the upper tropospheric upwelling? Alternatively, warmer sea surface temperatures in the tropics enhances convection and the meridional circulation's poleward advection of angular momentum, acting to strengthen the STJ. So, is this the mechanism by which the upper tropospheric upwelling response induces a strengthening of the STJ and the meridional temperature gradients follow suit?

Likewise, what aspects of the stratospheric response to CO₂ are or are not related to changes in the troposphere? Lin and Fu (2013) presents a thorough connection between the BDC acceleration and the increase in SSTs with anthropogenic forcing, indicating tropospheric changes are responsible for changes seen in the lower stratosphere. Chrysanthou et al. (2020) confirms a significant portion of the lower stratosphere's response to CO₂ is the result of global surface warming, yet there is also a rapid adjustment component indicating the lower stratosphere's ability to respond independent of tropospheric change. Additionally, studies note a downward control of the BDC's deep branch on its shallow branch (Haynes et al. 1991; Rosenlof and Holton 1993). Our results do not necessarily contradict the assertion that SST warming patterns may be significant in the response of lower stratospheric features. Rather, any connection may not involve the tropical upper tropospheric circulation response.

It's likely that both mechanisms listed above are at play but have differing contributions to the upper troposphere and the lower stratosphere. For instance, the enhanced convection in the troposphere may be more significant to the response of the upper tropospheric metrics whereas the increased thermal wind pattern may have more influence on the lower stratospheric metrics. Disentangling the impetus for the responses of tropospheric and stratospheric circulations may require carefully designed model experiments that isolate the changes to the coupled system.

Acknowledgments. The authors would like to acknowledge their collaboration with the International Space Science Institute (ISSI) in Bern, through ISSI International Team project 460, Tropical Width Impacts on the Stratosphere (TWIST). Helpful discussions at ISSI TWIST meetings improved the quality of this work. M.E.M. is supported by an appointment to the NASA Postdoctoral Program at the Goddard Institute for Space Studies, administered by Oak Ridge Associated Universities under contract with NASA. D.W.W. is supported by the U.S. National Science Foundation (NSF) award AGS-1902409. Climate modeling at GISS is supported by the NASA Modeling, Analysis and Prediction program, and resources supporting this work were provided by the NASA High-End Computing (HEC) Program through the NASA Center for Climate Simulation (NCCS) at Goddard Space Flight Center.

Data availability statement. The data used in this study is publicly available through Zenodo (https://doi.org/10.5281/zenodo.7324024). We are grateful to the GISS modeling groups for providing their model output.

References

Abalos, M., and Coauthors, 2020: Future trends in stratosphere-to-troposphere transport in CCMI models. *Atmospheric chemistry and physics*, **20** (**11**), 6883–6901.

Abalos, M., and Coauthors, 2021: The Brewer–Dobson circulation in CMIP6. *Atmospheric Chemistry and Physics*, **21** (**17**), 13 571–13 591.

Adam, O., and Coauthors, 2018: The TropD software package (v1): standardized methods for calculating tropical-width diagnostics. *Geoscientific Model Development*, **11** (**10**), 4339–4357.

Barnes, E. A., and L. Polvani, 2013: Response of the midlatitude jets, and of their variability, to increased greenhouse gases in the CMIP5 models. *Journal of Climate*, **26** (**18**), 7117–7135.

Bauer, S. E., and Coauthors, 2020: Historical (1850–2014) aerosol evolution and role on climate forcing using the GISS ModelE2. 1 contribution to CMIP6. *Journal of Advances in Modeling Earth Systems*, **12** (**8**), e2019MS001 978.

Birner, T., S. Davis, and D. Seidel, 2014: Earth's tropical belt. *Phys. Today*, 67 (12), 38–44.

- Butchart, N., and Coauthors, 2006: Simulations of anthropogenic change in the strength of the Brewer–Dobson circulation. *Climate Dynamics*, **27** (7), 727–741.
- Byrne, M. P., A. G. Pendergrass, A. D. Rapp, and K. R. Wodzicki, 2018: Response of the intertropical convergence zone to climate change: Location, width, and strength. *Current climate change reports*, **4** (**4**), 355–370.
- Chemke, R., and L. M. Polvani, 2019: Exploiting the Abrupt 4× CO2 Scenario to Elucidate Tropical Expansion Mechanisms. *Journal of Climate*, **32** (3), 859–875.
- Chrysanthou, A., A. C. Maycock, and M. P. Chipperfield, 2020: Decomposing the response of the stratospheric Brewer–Dobson circulation to an abrupt quadrupling in CO₂. *Weather and Climate Dynamics*, **1** (**1**), 155–174.
- Davis, N., and T. Birner, 2017: On the discrepancies in tropical belt expansion between reanalyses and climate models and among tropical belt width metrics. *Journal of Climate*, **30** (**4**), 1211–1231.
- Eichelberger, S. J., and D. L. Hartmann, 2005: Changes in the strength of the Brewer-Dobson circulation in a simple AGCM. *Geophysical research letters*, **32** (15).
- Eyring, V., S. Bony, G. A. Meehl, C. A. Senior, B. Stevens, R. J. Stouffer, and K. E. Taylor, 2016: Overview of the Coupled Model Intercomparison Project Phase 6 (CMIP6) experimental design and organization. *Geoscientific Model Development*, **9** (5), 1937–1958.
- Garcia, R. R., and W. J. Randel, 2008: Acceleration of the Brewer–Dobson circulation due to increases in greenhouse gases. *Journal of the Atmospheric Sciences*, **65** (8), 2731–2739.
- Grise, K. M., and L. M. Polvani, 2017: Understanding the Time Scales of the Tropospheric Circulation Response to Abrupt CO2 Forcing in the Southern Hemisphere: Seasonality and the Role of the Stratosphere. *Journal of Climate*, **30** (21), 8497–8515.
- Hardiman, S. C., N. Butchart, and N. Calvo, 2014: The morphology of the Brewer–Dobson circulation and its response to climate change in CMIP5 simulations. *Quarterly Journal of the Royal Meteorological Society*, **140** (**683**), 1958–1965.

- Haynes, P., M. McIntyre, T. Shepherd, C. Marks, and K. P. Shine, 1991: On the "downward control" of extratropical diabatic circulations by eddy-induced mean zonal forces. *Journal of the Atmospheric Sciences*, **48** (**4**), 651–678.
- Kelley, M., and Coauthors, 2020: GISS-E2. 1: Configurations and climatology. *Journal of Advances in Modeling Earth Systems*, **12** (**8**), e2019MS002 025.
- Kushner, P. J., I. M. Held, and T. L. Delworth, 2001: Southern Hemisphere atmospheric circulation response to global warming. *Journal of Climate*, **14** (**10**), 2238–2249.
- Lau, W. K., and K.-M. Kim, 2015: Robust Hadley circulation changes and increasing global dryness due to CO₂ warming from CMIP5 model projections. *Proceedings of the National Academy of Sciences*, **112** (**12**), 3630–3635.
- Li, F., R. S. Stolarski, S. Pawson, P. A. Newman, and D. Waugh, 2010: Narrowing of the upwelling branch of the Brewer-Dobson circulation and Hadley cell in chemistry-climate model simulations of the 21st century. *Geophysical research letters*, **37** (**13**).
- Lin, P., and Q. Fu, 2013: Changes in various branches of the Brewer–Dobson circulation from an ensemble of chemistry climate models. *Journal of Geophysical Research: Atmospheres*, **118** (1), 73–84.
- Menzel, M. E., D. Waugh, and K. Grise, 2019: Disconnect between Hadley cell and subtropical jet variability and response to increased CO2. *Geophysical Research Letters*, **46** (**12**), 7045–7053.
- Mitevski, I., C. Orbe, R. Chemke, L. Nazarenko, and L. M. Polvani, 2021: Non-Monotonic Response of the Climate System to Abrupt CO2 Forcing. *Geophysical Research Letters*, **48** (**6**), e2020GL090 861.
- Orbe, C., and Coauthors, 2020: GISS Model E2. 2: A Climate Model Optimized for the Middle Atmosphere—2. Validation of Large-Scale Transport and Evaluation of Climate Response. *Journal of Geophysical Research: Atmospheres*, **125** (**24**), e2020JD033 151.
- Rosenlof, K. H., 1995: Seasonal cycle of the residual mean meridional circulation in the stratosphere. *Journal of Geophysical Research: Atmospheres*, **100** (**D3**), 5173–5191.

- Rosenlof, K. H., and J. R. Holton, 1993: Estimates of the stratospheric residual circulation using the downward control principle. *Journal of Geophysical Research: Atmospheres*, **98** (**D6**), 10465–10479.
- Seidel, D. J., Q. Fu, W. J. Randel, and T. J. Reichler, 2008: Widening of the tropical belt in a changing climate. *Nature geoscience*, **1** (**1**), 21.
- Seviour, W. J., N. Butchart, and S. C. Hardiman, 2012: The Brewer–Dobson circulation inferred from ERA-Interim. *Quarterly Journal of the Royal Meteorological Society*, **138** (665), 878–888.
- Shaw, T. A., 2019: Mechanisms of future predicted changes in the zonal mean mid-latitude circulation. *Current Climate Change Reports*, **5** (**4**), 345–357.
- Shaw, T. A., and Z. Tan, 2018: Testing latitudinally dependent explanations of the circulation response to increased CO2 using aquaplanet models. *Geophysical Research Letters*, **45** (**18**), 9861–9869.
- Shepherd, T. G., and C. McLandress, 2011: A robust mechanism for strengthening of the Brewer–Dobson circulation in response to climate change: Critical-layer control of subtropical wave breaking. *Journal of the Atmospheric Sciences*, **68** (4), 784–797.
- Singh, M. S., and P. A. O'Gorman, 2012: Upward shift of the atmospheric general circulation under global warming: Theory and simulations. *Journal of Climate*, **25** (**23**), 8259–8276.
- Waugh, D. W., and Coauthors, 2018: Revisiting the relationship among metrics of tropical expansion. *Journal of Climate*, **31** (**18**), 7565–7581.